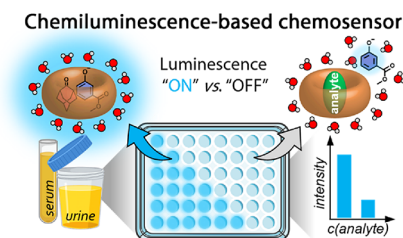


# Chemiluminescent Cucurbit[*n*]uril-Based Chemosensor for the Detection of Drugs in Biofluids

Nilima Manoj Kumar, Pierre Picchetti,\* Changming Hu, Laura M. Grimm, and Frank Biedermann\*

**ABSTRACT:** Chemiluminescence-based detection methods offer a superior signal-to-noise ratio and are commonly adopted for biosensors. This work presents the design and implementation of a supramolecular assay based on a chemiluminescent chemosensor. Specifically, an indicator displacement assay (IDA) with the supramolecular host–guest complex of chemiluminescent phenoxy 1,2-dioxetane and cucurbit[8]uril enables the low-micromolar detection of drugs in human urine and human serum samples. Cucurbit[8]uril thereby acts as a non-surfactant chemiluminescence enhancer and a synthetic receptor. Additionally, we show that adding an equimolar amount of cucurbit[8]uril to a commercially available dioxetane used in standard enzymatic chemiluminescence immunoassays enhances the chemiluminescence by more than 15 times. Finally, we demonstrate that a chemiluminescence resonance energy transfer between a unimolecular macrocyclic cucurbit[7]uril-dye conjugate and a phenoxy 1,2-dioxetane can be utilized to detect the herbicide paraquat at a micromolar concentration in aqueous media.

**KEYWORDS:** chemiluminescence, chemosensor, dioxetane, biofluids, cucurbit[*n*]uril



Supramolecular chemistry has enabled the design and preparation of artificial receptors that have potential applications in various fields such as environmental and medical diagnostics.<sup>1</sup> Chemosensors are functional receptor-like molecules that bind to analytes *via* non-covalent interactions and thereby produce a spectroscopically detectable signal, *e.g.*, a fluorescence response.<sup>2,3</sup> Like several other synthetic macrocyclic receptors,<sup>4–9</sup> cucurbit[*n*]urils (CB*n*)<sup>10</sup> are promising candidates for developing chemosensor-based diagnostic assays.<sup>11–15</sup> Specifically, CB*n* display outstanding binding affinities for many biomolecules and drugs<sup>16,17</sup> in aqueous solution ( $K_a \approx 10^3–10^9 \text{ M}^{-1}$ )<sup>18,19</sup> and are chemically stable, non-toxic,<sup>20</sup> water-soluble, and inexpensive to synthesize.<sup>21</sup> For fluorescent chemosensors, the spectroscopically active species, *e.g.*, reporter dyes, need to be excited by an external light source, leading to suboptimal signal-to-noise ratios in complex matrices. When applied to biofluids that contain emissive compounds and may be turbid, scattering and autofluorescence can negatively affect the performance of emission-based assays in clinical diagnostics.<sup>22,23</sup> In this respect, chemiluminescence (CL)-based sensing systems would be advantageous for the development of chemosensor-based assays because CL does not rely on an external light source to generate an emitting state but instead uses the inherent chemical energy of the “chemiluminescent fuel”.<sup>24</sup>

Various supramolecular CL-based systems have been converted into promising new materials such as light-on/light-off switches,<sup>25</sup> chemiluminescent hydrogels,<sup>26</sup> self-reporting polymers,<sup>27</sup> and agents for photodynamic therapy.<sup>28</sup> Likewise, CL-based signal readout is already in routine use for immunoassays in clinical diagnostics and pharmaceutical

research, providing ultralow sensitivity.<sup>29</sup> Chemiluminescent systems based on host–guest complexes have been described for hydrogen peroxide detection in water,<sup>30</sup> and the ability to image reactive oxygen species *in vitro* and *in vivo* has been reported.<sup>31</sup> However, no chemiluminescent host–guest-type chemosensors for sensing applications in biofluids of small organic molecules have been reported to the best of our knowledge.

Phenoxy 1,2-dioxetanes (PDOs) are widely utilized for CL-based assays,<sup>32–35</sup> *e.g.*, the ELISA-Light system. Conveniently, the conditions for generating CL from PDOs are compatible with multiple assay formats under physiologically relevant conditions. Moreover, many functionalized and protected PDOs have been developed whose CL is activated by particular enzymes, *e.g.*, alkaline phosphatase or  $\beta$ -galactosidase, which can be exploited to detect and image such enzymes at trace levels (enzyme-triggered CL).<sup>36</sup> Owing to solvent-induced quenching,<sup>37</sup> PDOs are characterized by relatively low CL quantum yields in polar media.<sup>38,39</sup> Recently, however, PDOs were successfully synthesized with a CL quantum yield of 9.8%.<sup>40</sup>

Performance enhancers, *i.e.*, surfactant-dye adducts, can increase luminescence intensity by confining the PDOs in an

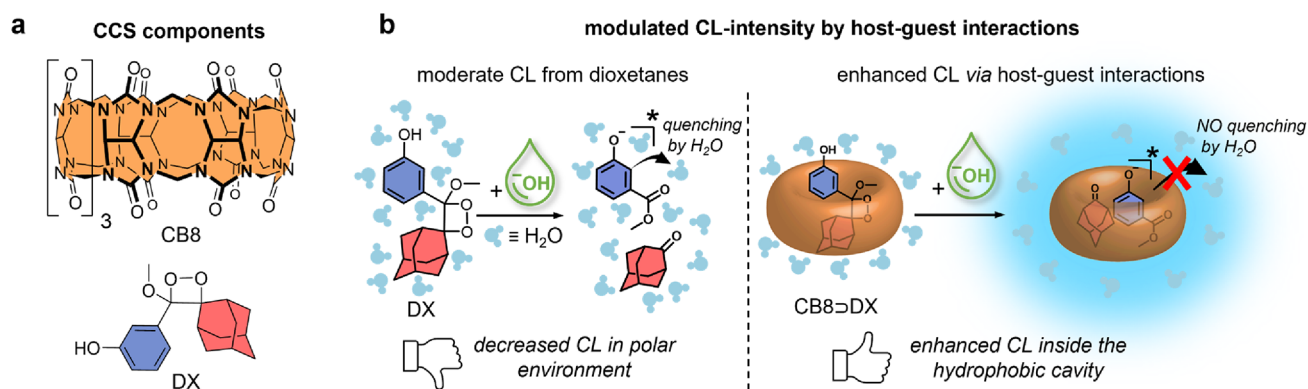


**Figure 1.** Schematic representation of the chemical structures and the role of host–guest interactions in modulating the CL properties of DX. (a) Chemical structures of the macrocyclic receptor CB8 and the chemiluminescent dioxetane DX. (b) Modulated CL of DX in the absence and presence of the macrocyclic receptor CB8.

apolar environment.<sup>41</sup> In addition, such surfactant-dye adducts enable energy transfer from the excited state of the chemiluminescent species to a more efficiently emitting acceptor fluorophore. However, performance-enhancers based on surfactants or surfactant-dye conjugates can be chemically unstable and problematic for imaging in living cells.<sup>42</sup> Consequently, it is of great interest to develop alternative, non-surfactant-based performance-enhancers for chemiluminescent PDOs.

In this work, we report a chemiluminescence-based chemosensor (CCS) assay for the detection of drugs at low micromolar concentrations in biofluids, *i.e.*, human urine and human serum, using a structurally simple PDO, namely 3-(4-methoxyspiro[1,2-dioxetane-3,2'-tricyclo[3.3.1.1<sup>3,7</sup>]decan]-4-yl)phenol (DX; Figure 1a). Moreover, we demonstrate that the biocompatible and commercially available macrocycle cucurbit[8]uril (CB8) functions as a non-surfactant CL performance enhancer (Figure 1b) in addition to being a receptor. Furthermore, we show that the CB8-dependent CL enhancement is suitable for commercially available PDOs. Finally, we explore the possibility of detecting the herbicide paraquat *via* chemiluminescence resonance energy transfer (CRET) using a cucurbit[7]uril (CB7)-dye conjugate.

## RESULTS AND DISCUSSION

**Chemiluminescent Properties of DX and Its Host–Guest Inclusion Complex with CB8.** Chemiluminescent PDOs (see Figures 1 and 4 for their chemical structures) attracted our attention as potentially suitable reporter dyes for CB $n$  ( $n = 7, 8$ ) as they contain a CB $n$ -binding adamantane moiety. Due to the strong binding of 1-adamantanol to CB7 ( $\log K_a = 10.4$ ) and CB8 ( $\log K_a = 6.8$ ) in water,<sup>43</sup> we also expected that suitable PDOs are efficiently complexed by this host family in the micromolar concentration regime in aqueous media. Thus, DX was prepared following literature procedures (see Supporting Information).<sup>40,44</sup> Compound DX is long-term stable for at least 1 h in acidic aqueous solutions (pH 6.0; Figure S1a) but undergoes chemical transformation and displays a blue CL emission when the pH is increased to 9.6 ( $\lambda_{\text{em,max}} = 471$  nm, Figure S1b–d). This base-triggered CL takes place after deprotonation of the phenol moiety ( $\text{p}K_a \approx 9.0$ ) of DX, leading to the formation of an electronically excited phenoxy methyl ester intermediate, E\* (Figure S1e).<sup>24,33</sup>

As anticipated, DX forms a strong host–guest inclusion complex with CB8 (CB8 $\supset$ DX,  $\log K_{a,\text{CB8}\supset\text{DX}} = 6.2$ ), as was assessed by a fluorescent dye displacement assay in 10 mM PBS at pH 6.0 (Figure S2). In addition, the host–guest complex formation was confirmed by mass spectrometry (Figure S3).

When triggering the CL reaction of DX through NaOH addition, we found a 4.5-fold enhancement of CL intensity ( $\lambda_{\text{max}} = 455$  nm) for the CB8 $\supset$ DX complex compared to the free DX ( $\lambda_{\text{max}} = 471$  nm) at pH 9.6 in 10 mM PBS (Figure 2b, IV, from the black curve to the blue curve). The observed CL enhancement can be explained as CB8 accommodates both the adamantanone and the electronically excited state of the phenoxy derivative (E\*). Inside the CB8 cavity, the phenoxy derivative is protected from deactivation (Figure 1b): Mechanistically, the observed enhancement of the CL intensity indicates that the excited chromophore, generated upon base addition, remains confined within the receptor cavity and is thus protected from the surrounding water molecules. Indeed, the CL arising from the CB8 $\supset$ DX host–guest complex shows a hypsochromic shift ( $\Delta = 16$  nm, Figure S4a) of the emission wavelength maximum compared to that of free DX, supporting the inclusion complex hypothesis.<sup>45</sup> The reproducibility of the CL enhancement effect was confirmed by six replica measurements, yielding a very good relative standard deviation (RSD) of only 4% (Figure S4b).

For comparison, methylated  $\beta$ -cyclodextrin derivatives can also be used as non-surfactant additives for CL enhancement of 1,2-dioxetanes.<sup>31,46</sup> However, they require a much higher host concentration (at least 5-fold concentration excess) to ensure a sufficient degree of dioxetane complexation, rendering them suboptimal for the micromolar detection of most drugs and biomolecules. Non-methylated cyclodextrins are even CL quenchers.<sup>31</sup>

**Chemiluminescent Detection of Mem and Nan.** Due to the high affinity and sizable CL enhancement effect provided by CB8, this host appeared to be a promising candidate for developing a CL-based supramolecular assay that is operational in aqueous media and biofluids. CB8 has a high binding affinity for the hydrophobic drugs memantine (Mem,  $\log K_a = 12.9$ )<sup>11</sup> and nandrolone (Nan,  $\log K_a = 7.3$ ),<sup>47</sup> the former being a medication for the treatment of Alzheimer's disease<sup>48</sup> and the latter being a synthetic anabolic steroid (Figure 2a).<sup>49</sup> As such, we expected these high-affinity drugs to displace the chemiluminescent reporter DX from the cavity of

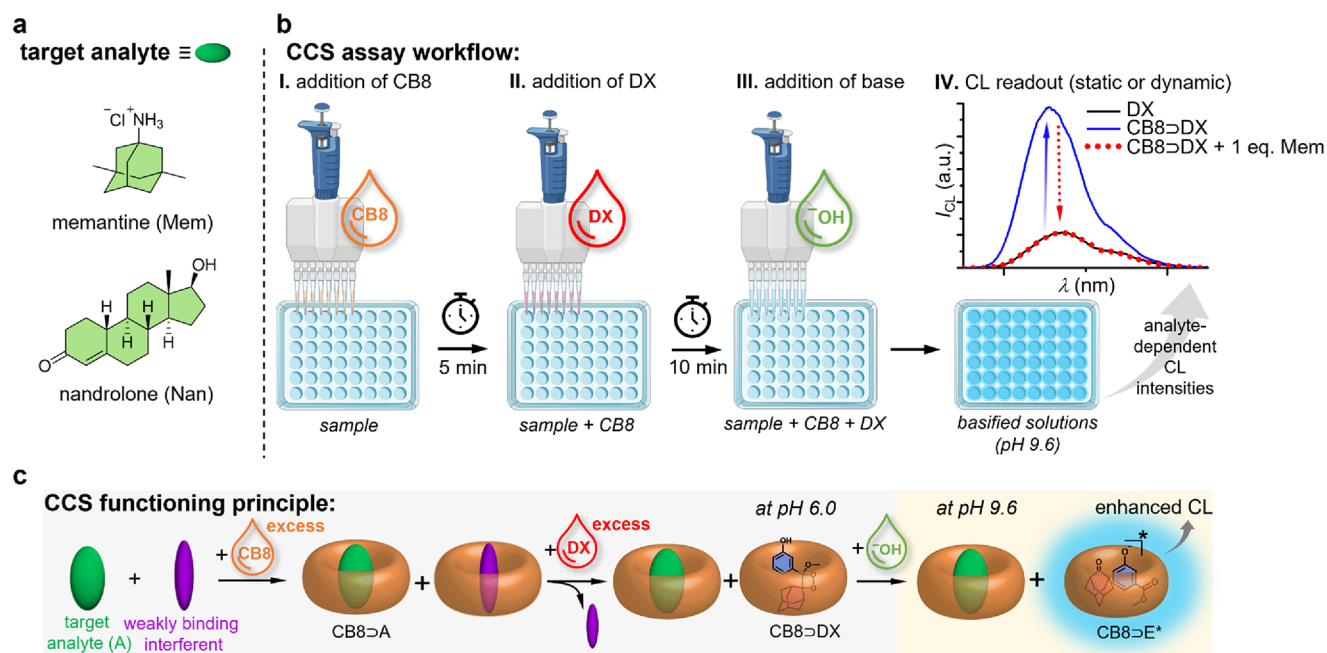


**Figure 2.** Chemical structures of the target analytes and schematic representation of the implementation and functioning principle of the herein presented assay. (a) Chemical structures of the analytes Mem and Nan. (b) Schematic representation of the chemiluminescence-based chemosensor (CCS) assay. The graph shows the Mem-dependent decrease in the CL intensity ( $[\text{Mem}] = 30 \mu\text{M}$ ,  $[\text{CB8}] = 30 \mu\text{M}$ , and  $[\text{DX}] = 30 \mu\text{M}$ ) in 10 mM PBS at pH 9.6. (c) Schematic representation of the functioning principle of CCS.

CB8, consequently reducing the CL signal and affecting the luminescence kinetics. The schematic workflow for the CCS assay is depicted in Figure 2b (see also the Materials and Methods). In the first step, CB8 ( $30 \mu\text{M}$ ) is added to an aqueous solution (pH 6.0) of the analyte (A), e.g., Mem. After a short equilibration time (5 min) in which the spectroscopically silent receptor–analyte complex ( $\text{CB8>A}$ , Figure 2c) forms, an equimolar amount of DX ( $30 \mu\text{M}$  final concentration in the assay medium) is added. DX sequesters the remaining unoccupied CB8 by forming the corresponding  $\text{CB8>DX}$  complex (Figure 2c). Compared to the binding affinities of CB8 with Mem or Nan, the lower affinity of DX ensures that no analyte is displaced from  $\text{CB8>A}$  once it is added to the solution. However, weaker CB8-binding interferents in the biofluid matrix, such as metabolites, is displaced from the CB8 cavity by DX, which is a desirable side effect of the assay setup. The CL reaction is subsequently triggered by the fast addition of base ( $\text{NaOH}_{\text{aq}}$ ) into the microplate well, and the kinetic emission profiles are recorded by collecting all the light (320–740 nm). Specifically, a gradual decrease in the onset of CL (Figure S5) was observed when CB8 ( $30 \mu\text{M}$ ) was premixed with Mem-containing ( $0\text{--}60 \mu\text{M}$ ) samples in PBS (10 mM) prior to the addition of DX ( $30 \mu\text{M}$ ), whereas the presence of an equimolar amount of Mem resulted in no enhancement of CL intensity (Figure 2b, IV, dotted curve). Comparable results were obtained for the detection of Nan ( $0\text{--}60 \mu\text{M}$ ) in PBS (10 mM); the CL intensity decreased with increasing Nan concentration in the sample (Figure S6). For visualization purposes and to guide the eye, we have fitted the concentration plots for Mem and Nan with an exponential decay fitting curve.

Unlike some antibody-based assays that require lengthy equilibration times,<sup>50</sup> our supramolecular chemiluminescent assay can be carried out rapidly and without peculiar precautions: Indeed, studies on the effect of the equilibration time (set between 5 and 20 min) of premixing Mem with CB8

showed no significant effect on the final CL intensity (Figure S7). In accordance with the proposed mechanism of the CCS, the detection of Mem or Nan was not successful when DX was used without CB8 (Figure S8).

Notably, the detection of Mem (Figure 3a–d) and Nan (Figure S9a–d) was also possible in deproteinized human serum (1:3 diluted with 10 mM PBS at pH 6.0) and human urine (1:1 diluted with 10 mM PBS at pH 6.0). As pointed out before, the addition of DX to the CB8-spiked biofluid specimen causes the desirable displacement of more weakly binding interferents from the hosts' cavity while not affecting the integrity of the  $\text{CB8>A}$  complexes. The therapeutic range of Mem in plasma varies between 0.50 and  $0.83 \mu\text{M}$ , with a toxicity level set at  $1.67 \mu\text{M}$ .<sup>51</sup> Because the CCS can detect Mem at concentrations as low as  $1 \mu\text{M}$ , our chemiluminescent assay may be further developed to detect Mem overdoses or inappropriate drug administration in Alzheimer's disease patients (as dementia is the main symptom of this disease; this patient group is particularly subject to abnormal drug intake).<sup>52</sup> In addition, Nan levels are monitored by anti-doping agencies in sports competitions, and abuse can be detected by Nan levels greater than 7 and 18 nM in female and male athletes, respectively.<sup>53</sup> Although our CCS currently cannot achieve nanomolar sensitivity, it is operational in the micromolar concentration range. Thus, it may be used for the rapid on-site detection of Nan in illicit preparations used by athletes before or during competitions.

**CB8 as CL Enhancer for the Commercially Available Dioxetane CDP-Star.** Furthermore, the CB8-based CL enhancement is not limited to dioxetane DX but can also be utilized for the commercially available CDP-Star dioxetane substrate (Figure 4a), which has already found practical uses for, e.g., enzyme-linked immunosorbent assays.<sup>38,54</sup> We found that equimolar addition of CB8 ( $30 \mu\text{M}$ ) to a solution of enhancer-free CDP-Star ( $30 \mu\text{M}$  in 10 mM Tris–HCl buffer

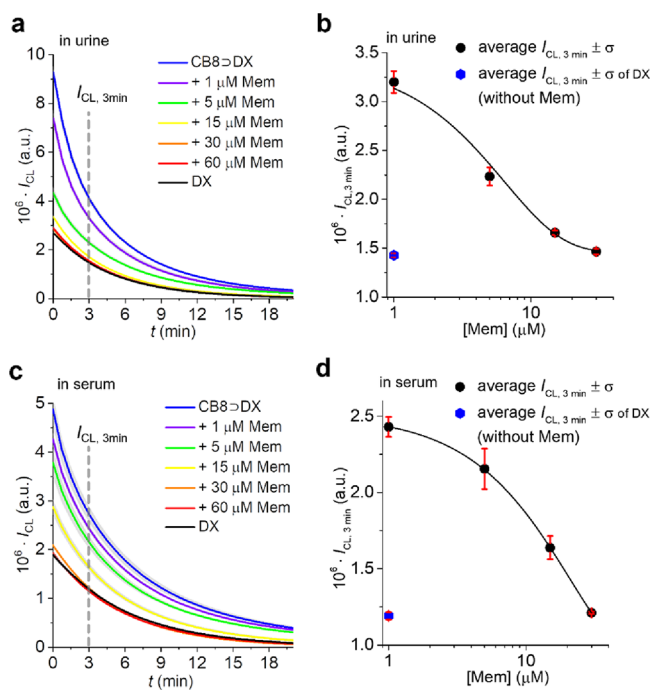


**Figure 3.** Sensing of analytes in urine and serum. (a) Time-dependent CL response of CCS ([CB8] = 30  $\mu$ M and [DX] = 30  $\mu$ M; pH 9.6) in Mem-spiked (0–60  $\mu$ M) diluted urine (1:1 with 10 mM PBS; containing 2.5 vol% DMSO) and (b) semi-log plot of the corresponding CL intensities ( $I_{CL}$ ) plotted at 3 min after the addition of NaOH<sub>aq</sub> (10 mM, 10  $\mu$ L). (c) Time-dependent CL response of CCS ([CB8] = 30  $\mu$ M and [DX] = 30  $\mu$ M; pH 9.6) in Mem-spiked deproteinized human serum (diluted 1:3 with 10 mM PBS; containing 2.5 vol% DMSO) and (d) semi-log plot of the corresponding  $I_{CL}$  plotted at 3 min after the addition of NaOH<sub>aq</sub> (10 mM, 10  $\mu$ L). The average  $I_{CL}$  and the corresponding standard deviation ( $\sigma$ ) were calculated from six independent measurements.

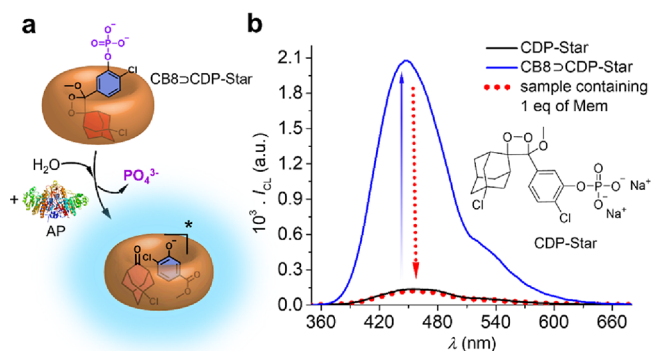


**Figure 4.** Implementation of CB8-based CL amplification for the commercially available, enzyme-responsive CDP-Star. (a) Schematic representation of the AP-catalyzed dephosphorylation of CB8 $\rightarrow$ CDP-Star, resulting in an enhanced CL due to host–guest complexation. (b) CL emission spectra of CDP-Star in the presence and absence of CB8 in 10 mM Tris–HCl buffer solution containing 1 mM Mg<sup>2+</sup> and 3 U mL<sup>-1</sup> of AP at 37 °C (pH 9.0). Also shown is the CL emission when 1 eq of Mem was added to CDP-Star prior to CB8 and enzyme addition.

solution containing 1 mM Mg<sup>2+</sup> and 3 U mL<sup>-1</sup> of alkaline phosphatase (AP) at 37 °C, pH 9.0) resulted in a 15-fold increase in the CL intensity (Figure 4b). For the reasons described above, no enhancement of CL intensity was observed when CB8 was premixed with an equimolar amount

of Mem before the addition of CDP-Star. Notably, the addition of  $\beta$ -CD to CDP-Star did not enhance CL but even resulted in pronounced quenching (Figure S10),<sup>31</sup> again highlighting the superior performance of CB8 as a macrocyclic CL enhancer.

**CRET Study between DX and CB7-CF.** DX also forms a relatively strong inclusion complex with the smaller CB7 homologue ( $\log K_{a, \text{CB7} \rightarrow \text{DX}} = 7.2$  in water at pH 6.0), as was assessed by a fluorescent dye displacement assay (Figure S11). In saline media, this affinity is significantly reduced.<sup>55,56</sup> Despite their apparent similarity, CB7 $\rightarrow$ DX and CB8 $\rightarrow$ DX remarkably differ in terms of CL properties. For example, no CL enhancement was observed with CB7 $\rightarrow$ DX in basic media (Figure S12). The smaller cavity of CB7 probably accommodates only the adamantane moiety but not the chromophore of DX, and thus, the DX binding moiety remains exposed to surrounding water molecules (Figure S13), resulting in the deactivation process as mentioned above.

Nevertheless, CRET<sup>31</sup> can be realized for sensing applications by using a suitable CB7-dye conjugate as host. For this purpose, the CRET-acceptor carboxyfluorescein azide (CF-N<sub>3</sub>) was covalently linked to CB7 (CB7-CF, Figure 5a) by following literature procedures (see the Supporting Information).<sup>57</sup> CF-N<sub>3</sub> displays a strong spectral overlap between its absorption profile and the emission profile of DX (CRET donor; Figure 5b), which will also be the case for CB7-CF. Indeed, after the formation of CB7-CF $\rightarrow$ DX (Figure 5c, I) and subsequent basification, CRET was observed as indicated by the CB7-CF-sensitized and dependent emission, whereas a concomitant CL intensity reduction of DX was also witnessed (Figure 5d; see Materials and Methods). Furthermore, the importance of the macrocyclic binding motif in CB7-CF, which serves as an anchor point for the binding of DX, was confirmed by the control experiment in which the dye CF-N<sub>3</sub> and DX alone were studied for CRET; in this case, a lower (50%) CRET intensity was observed (Figure S14a).

**CRET-Based Detection of Methyl Viologen.** Finally, we investigated the possibility of utilizing the above-described CRET-process for sensing methyl viologen (MV<sup>2+</sup>,  $\log K_{a, \text{CB7}} = 7.4$  in water; Figure 5a)<sup>58</sup>—a herbicide known to be associated with the development of Parkinson’s disease.<sup>59</sup> For this purpose, we followed the CRET process occurring in MV<sup>2+</sup>-spiked water samples (see the Materials and Methods). As a result, we found that increasing amounts of MV<sup>2+</sup> caused CRET quenching (Figure 5e). Thus, micromolar detection of the herbicide viologen by a ratiometric method is possible in aqueous solutions using a chemiluminescent chemosensor ensemble. Mechanistically, MV<sup>2+</sup> most probably acts as an electron transfer (eT) quencher for DX and CB7-CF (Figure 5c, II),<sup>60,61</sup> as was deduced by additional control experiments (see the Supporting Information).

**General Discussion on Current Limitations and Performance of the CCS Assay.** CB $n$  show high binding affinities for many biomolecules and are therefore rather unselective binders. Thus, the CCS presented in this work is at this point limited to the detection of high-affinity drugs such as Mem and Nan. Previous works using fluorescent CB $n$ -based chemosensing ensembles reported the detection of Nan (0–43.2  $\mu$ M) in PBS<sup>55</sup> and Mem (0–2  $\mu$ M) in spiked human serum.<sup>11</sup> However, to reduce the disturbances from the autofluorescence background, a sensitive fluorimeter in combination with 3 mL cuvettes had to be used for experiments in blood serum. Both Nan and Mem can also be detected in the micromolar concentration range with the

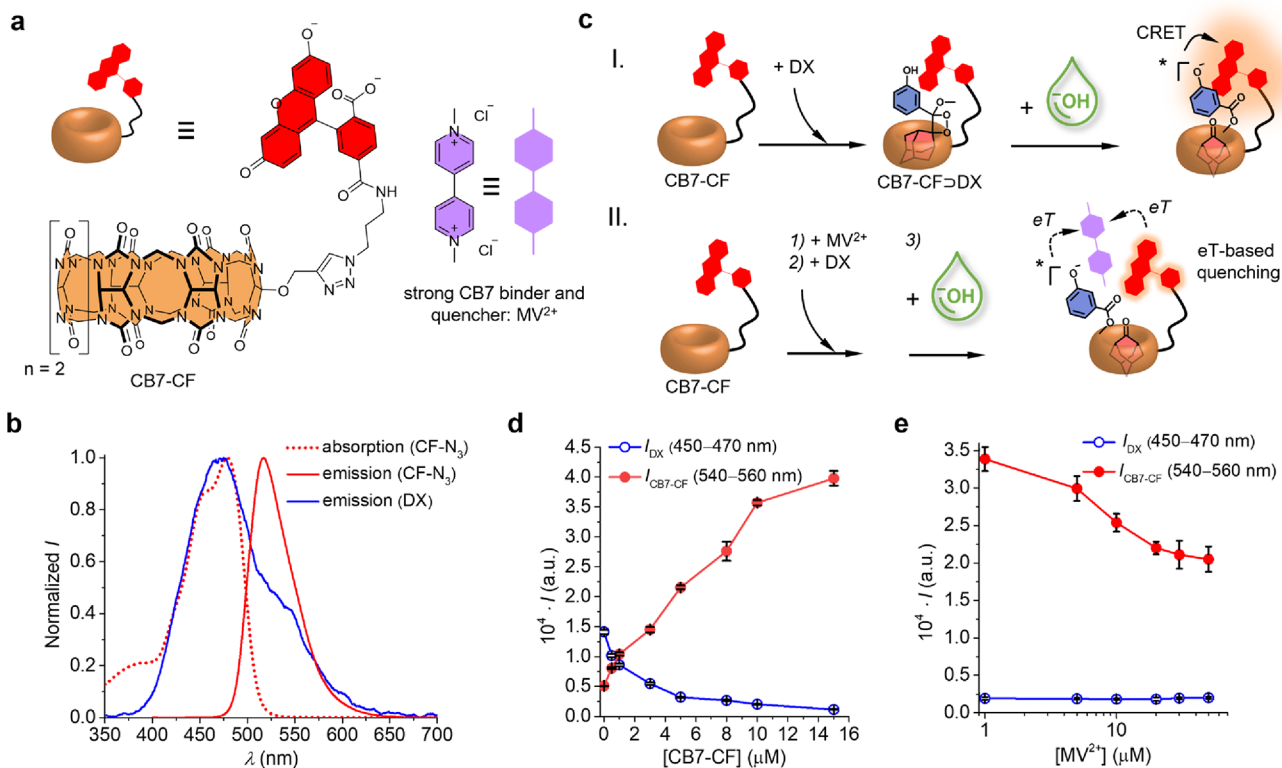


**Figure 5.** CRET studies. (a) Chemical structures of CB7-CF and MV<sup>2+</sup>. (b) Normalized absorption ( $\lambda_{\text{CF-N}_3/\text{abs,max}} = 477 \text{ nm}$ ) and emission profiles of the acceptor dye CF-N<sub>3</sub> ( $\lambda_{\text{ex}} = 477 \text{ nm}$ ;  $\lambda_{\text{CF-N}_3/\text{em,max}} = 520 \text{ nm}$ ) in water. The normalized CL spectrum of DX at pH 9.6 in water is also shown. (c) Schematic representation of the binding mechanism and CRET process between DX and CB7-CF in the absence and presence of MV<sup>2+</sup>. (d) CB7-CF-dependent CRET luminescence intensities with DX (10  $\mu\text{M}$  in water containing 2.8 vol% DMSO, pH 9.6). (e) CRET luminescence intensities ([DX] = 10  $\mu\text{M}$  and [CB7-CF] = 10  $\mu\text{M}$  in water containing 2.8 vol% DMSO, pH 9.6) at different MV<sup>2+</sup> concentrations. The average emission intensities and the corresponding standard deviation ( $\sigma$ ) were calculated from five independent measurements.

CCS. The limit of detection (LOD) for Mem (Figure S16) and Nan (Figure S17) in PBS, urine, and serum samples was determined from the linear-response range of the CCS calibration curve and is summarized in Table S1. Since host-guest interactions follow nonlinear relationships, the LOD calculated using general linear regression is considered to be only approximative. Nevertheless, the results show that the CCS can be used to detect low micromolar quantities of the drugs Mem and Nan. As a significant advance of the state of the art, a microplate reader can execute the CCS assay in a high-throughput and low-volume format even in human urine and human serum due to the efficient fluorescence background elimination.

To evaluate the performance of the CCS under the influence of matrix-to-matrix effects, we performed recovery studies using Mem-spiked urine samples from three healthy voluntary donors. In addition, a previously reported fluorescence-based indicator displacement assay (IDA) for Mem that is compatible with biofluids was utilized for validation of the CCS.<sup>11</sup> As shown in Tables S2 and S3, the CCS showed good recoveries (>85%) in all the samples tested, including spiked urine, and yielded comparable analyte concentration values as the IDA. Unlike the IDA, the CCS is not affected by the fluorescence background from the media.

## CONCLUSIONS

In summary, we have presented a novel chemiluminescence-based chemosensor assay for the detection of drugs in saline media and real biofluids at low-micromolar concentrations. To

this end, CB8 was shown to serve as a versatile chemiluminescent enhancer of adamantyl-bearing 1,2-dioxetanes. The herein presented methodology is readily adaptable to enzyme-coupled chemiluminescence assays with commercially available dioxetanes and has the potential to improve chemiluminescence-based diagnostic assays by providing a simpler, non-toxic, and more cost-efficient alternative to polymer-based performance enhancers. Moreover, chemiluminescence resonance energy transfer can be achieved by combining dioxetanes with suitable dye-CB7 conjugates, giving further opportunities to tune the dioxetane-based assay, e.g., for the CRET-based detection of herbicides in water.

## MATERIALS AND METHODS

Refer to the Supporting Information for full protocols, descriptions, ethical approval, and informed consent. For information on data uploaded to open repositories, see the associated content.

**CCS Assay Procedure.** In a typical procedure, the analyte spiked (0–60  $\mu\text{M}$ ) PBS stock solution or diluted urine (1:1) with 10 mM PBS (pH 6.0) or diluted (1:3) deproteinized serum with 10 mM PBS (pH 6.0) was added to a well of a 96-well Optiplate. The CB8 stock solution (typically 300  $\mu\text{M}$  in Milli-Q water) was then added, and the mixture was left at static conditions at room temperature for 5 min. Then, DX, dissolved in DMSO (typically a 1 mM stock solution), was added to the mixture, and the solution was left at static conditions for another 10 min after mixing (Note: the volume taken from each stock solution was chosen so that the final concentration of CB8 and DX present in one well was 30  $\mu\text{M}$  each). CL was induced by adding NaOH<sub>aq</sub> (10 mM solution, 10  $\mu\text{L}$ ), and the reaction mixture was briefly shaken (20 s) using a plate reader built-in shaking device. The

final volume of the test mixture of one well was 200  $\mu\text{L}$  and contained 2.5 vol% DMSO from the addition of DX. The CL intensity (whole wavelength range) was recorded immediately after shaking.

**CRET Assay between DX and CB7-CF.** To a solution of CB7-CF (0–15  $\mu\text{M}$ ) in Milli-Q water (pH 6.0) placed in a 96-well Optiplate, DX (10  $\mu\text{M}$ ) was added. CL was subsequently triggered by adding  $\text{NaOH}_{\text{aq}}$  (10 mM solution, 10  $\mu\text{L}$ ), and the reaction mixture was briefly shaken (20 s) using a plate reader built-in shaking device. The final volume of the mixture in the well was 200  $\mu\text{L}$  and contained 2.8 vol% DMSO. After shaking (20 s), luminescence intensities in the wavelength ranges of 450–470 nm and 540–560 nm, corresponding to DX and CB7-CF, respectively, were recorded. Likewise, the same protocol was followed between CF- $\text{N}_3$  and DX.

**CRET Experiments in the Presence of  $\text{MV}^{2+}$ .**  $\text{MV}^{2+}$ -spiked solutions (0–50  $\mu\text{M}$  in Milli-Q water, pH 6.0) were added to a well of a 96-well Optiplate. Subsequently, aliquots of the CB7-CF stock solution (in Milli-Q water, pH 6.0) were added so that the final concentration of CB7-CF in the microwell was 10  $\mu\text{M}$ . The mixture was left at static conditions at room temperature for 2–3 min. Then DX, dissolved in DMSO, was added so that its final concentration in the well plate was 10  $\mu\text{M}$ , and the solution was mixed well. After mixing, CL was triggered by adding  $\text{NaOH}_{\text{aq}}$  (10 mM solution, 10  $\mu\text{L}$ ), and the reaction mixture was briefly shaken (20 s) using a plate reader built-in shaking device. The final volume of the mixture in one well was 200  $\mu\text{L}$  and contained 2.8 vol% DMSO. After shaking, the luminescence intensities in the wavelength ranges of 450–470 nm and 540–560 nm, corresponding to DX and CB7-CF, respectively, were recorded. Likewise, the same protocol was followed between CF- $\text{N}_3$  and DX.

## ■ ASSOCIATED CONTENT

### ● Supporting Information

The Supporting Information is available free of charge at <https://pubs.acs.org/doi/10.1021/acssensors.2c00934>.

Details about instruments, materials and methods, binding affinity studies, chemiluminescence experiments, CRET experiments, and chemical synthesis (PDF)

## ■ AUTHOR INFORMATION

### Corresponding Authors

**Pierre Picchetti** – Karlsruhe Institute of Technology (KIT), Institute of Nanotechnology (INT), 76344 Eggenstein-Leopoldshafen, Germany; [orcid.org/0000-0002-0689-5998](https://orcid.org/0000-0002-0689-5998); Email: [pierre.picchetti@kit.edu](mailto:pierre.picchetti@kit.edu)

**Frank Biedermann** – Karlsruhe Institute of Technology (KIT), Institute of Nanotechnology (INT), 76344 Eggenstein-Leopoldshafen, Germany; [orcid.org/0000-0002-1077-6529](https://orcid.org/0000-0002-1077-6529); Email: [frank.biedermann@kit.edu](mailto:frank.biedermann@kit.edu)

### Authors

**Nilima Manoj Kumar** – Karlsruhe Institute of Technology (KIT), Institute of Nanotechnology (INT), 76344 Eggenstein-Leopoldshafen, Germany

**Changming Hu** – Karlsruhe Institute of Technology (KIT), Institute of Nanotechnology (INT), 76344 Eggenstein-Leopoldshafen, Germany; [orcid.org/0000-0002-1220-003X](https://orcid.org/0000-0002-1220-003X)

**Laura M. Grimm** – Karlsruhe Institute of Technology (KIT), Institute of Nanotechnology (INT), 76344 Eggenstein-Leopoldshafen, Germany; [orcid.org/0000-0002-1808-2206](https://orcid.org/0000-0002-1808-2206)

Complete contact information is available at: <https://pubs.acs.org/10.1021/acssensors.2c00934>

## Author Contributions

The manuscript was written with the contributions of all authors. All authors have approved the final version of the manuscript.

## Notes

The authors declare no competing financial interest.

## ■ ACKNOWLEDGMENTS

N. M. K. acknowledges the German Academic Exchange Service (DAAD) for financial support. C. H. acknowledges the China Scholarship Council (No. 201806920036). P. P. and F. B. acknowledge the Emmy Noether program of the Deutsche Forschungsgemeinschaft (BI-1805/2-1) for financial support. L.M.G. and F.B. acknowledge the Vector Stiftung for financial support (P2020-0135). The authors thank Papri Chakraborty (KIT-INT) for her kind support during mass spectrometry data acquisition.

## ■ ABBREVIATIONS

CB7, cucurbit[7]uril; CB8, cucurbit[8]uril; CCS, chemiluminescence-based chemosensor; CF- $\text{N}_3$ , carboxyfluorescein azide; CL, chemiluminescence; CRET, chemiluminescence resonance energy transfer; DMSO, dimethyl sulfoxide; DX, 3-(4-methoxy Spiro[1,2-dioxetane-3,2'-tricyclo[3.3.1.1<sup>3,7</sup>]decan-4-yl)phenol; eT, electron transfer; LOD, limit of detection; Mem, memantine;  $\text{MV}^{2+}$ , methyl viologen; Nan, nandrolone; PBS, phosphate-buffered saline; PDO, phenoxy 1,2-dioxetane

## ■ REFERENCES

- (1) You, L.; Zha, D.; Anslyn, E. V. Recent Advances in Supramolecular Analytical Chemistry Using Optical Sensing. *Chem. Rev.* **2015**, *115*, 7840–7892.
- (2) Bell, T. W.; Hext, N. M. Supramolecular Optical Chemosensors for Organic Analytes. *Chem. Soc. Rev.* **2004**, *33*, 589–598.
- (3) Bhasikuttan, A. C.; Pal, H.; Mohanty, J. Cucurbit[n]uril Based Supramolecular Assemblies: Tunable Physico-Chemical Properties and Their Prospects. *Chem. Commun.* **2011**, *47*, 9959–9971.
- (4) Ueno, A.; Kuwabara, T.; Nakamura, A.; Toda, F. A Modified Cyclodextrin as a Guest Responsive Colour-Change Indicator. *Nature* **1992**, *356*, 136–137.
- (5) Serio, N.; Moyano, D. F.; Rotello, V. M.; Levine, M. Array-Based Detection of Persistent Organic Pollutants via Cyclodextrin Promoted Energy Transfer. *Chem. Commun.* **2015**, *51*, 11615–11618.
- (6) Ogoshi, T.; Hashizume, M.; Yamagishi, T. A.; Nakamoto, Y. Synthesis, Conformational and Host-Guest Properties of Water-Soluble Pillar[5]arene. *Chem. Commun.* **2010**, *46*, 3708–3710.
- (7) Dai, D.; Li, Z.; Yang, J.; Wang, C.; Wu, J. R.; Wang, Y.; Zhang, D.; Yang, Y. W. Supramolecular Assembly-Induced Emission Enhancement for Efficient Mercury(II) Detection and Removal. *J. Am. Chem. Soc.* **2019**, *141*, 4756–4763.
- (8) Bauer, L. J.; Gutsche, C. D. Calixarenes. 15. The Formation of Complexes of Calixarenes with Neutral Organic Molecules in Solution. *J. Am. Chem. Soc.* **1985**, *107*, 6063–6069.
- (9) Guo, D.-S.; Uzunova, V. D.; Su, X.; Liu, Y.; Nau, W. M. Operational Calixarene-Based Fluorescent Sensing Systems for Choline and Acetylcholine and Their Application to Enzymatic Reactions. *Chem. Sci.* **2011**, *2*, 1722–1734.
- (10) Kim, J.; Jung, I.-S.; Kim, S.-Y.; Lee, E.; Kang, J.-K.; Sakamoto, S. Y. K.; Kim, K. New Cucurbituril Homologues: Syntheses, Isolation, Characterization, and X-ray Crystal Structures of Cucurbit[n]uril (n = 5, 7, and 8). *J. Am. Chem. Soc.* **2000**, *122*, 540–541.
- (11) Sinn, S.; Spuling, E.; Bräse, S.; Biedermann, F. Rational Design and Implementation of a Cucurbit[8]uril-Based Indicator-Displacement Assay for Application in Blood Serum. *Chem. Sci.* **2019**, *10*, 6584–6593.

- (12) Praetorius, A.; Bailey, D. M.; Schwarzlose, T.; Nau, W. M. Design of a Fluorescent Dye for Indicator Displacement from Cucurbiturils: A Macrocyclic Responsive Fluorescent Switch Operating Through a pKa Shift. *Org. Lett.* **2008**, *10*, 4089–4092.
- (13) Minami, T.; Esipenko, N. A.; Akdeniz, A.; Zhang, B.; Isaacs, L.; Anzenbacher, P., Jr. Multianalyte Sensing of Addictive Over-the-Counter (OTC) Drugs. *J. Am. Chem. Soc.* **2013**, *135*, 15238–15243.
- (14) Biedermann, F.; Hathazi, D.; Nau, W. M. Associative Chemosensing by Fluorescent Macrocyclic-Dye Complexes - a Versatile Enzyme Assay Platform Beyond Indicator Displacement. *Chem. Commun.* **2015**, *51*, 4977–4980.
- (15) Sinn, S.; Krämer, J.; Biedermann, F. Teaching Old Indicators Even More Tricks: Binding Affinity Measurements with the Guest-Displacement Assay (GDA). *Chem. Commun.* **2020**, *56*, 6620–6623.
- (16) Saleh, N.; Koner, A. L.; Nau, W. M. Activation and Stabilization of Drugs by Supramolecular pKa Shifts: Drug-Delivery Applications Tailored for Cucurbiturils. *Angew. Chem., Int. Ed.* **2008**, *47*, 5398–5401.
- (17) Konda, S. K.; Maliki, R.; McGrath, S.; Parker, B. S.; Robinson, T.; Spurling, A.; Cheong, A.; Lock, P.; Pigram, P. J.; Phillips, D. R.; Wallace, L.; Day, A. I.; Collins, J. G.; Cutts, S. M. Encapsulation of Mitoxantrone within Cucurbit[8]uril Decreases Toxicity and Enhances Survival in a Mouse Model of Cancer. *ACS Med. Chem. Lett.* **2017**, *8*, 538–542.
- (18) Sinn, S.; Biedermann, F. Chemical Sensors Based on Cucurbit[n]uril Macrocycles. *Isr. J. Chem.* **2018**, *58*, 357–412.
- (19) Biedermann, F.; Uzunova, V. D.; Scherman, O. A.; Nau, W. M.; De Simone, A. Release of High-Energy Water as an Essential Driving Force for the High-Affinity Binding of Cucurbit[n]urils. *J. Am. Chem. Soc.* **2012**, *134*, 15318–15323.
- (20) Uzunova, V. D.; Cullinane, C.; Brix, K.; Nau, W. M.; Day, A. I. Toxicity of Cucurbit[7]uril and Cucurbit[8]uril: An Exploratory In Vitro and In Vivo Study. *Org. Biomol. Chem.* **2010**, *8*, 2037–2042.
- (21) Koner, A. L.; Nau, W. M. Cucurbituril Encapsulation of Fluorescent Dyes. *Supramol. Chem.* **2007**, *19*, 55–66.
- (22) Simeonov, A.; Davis, M. I., *Interference with Fluorescence and Absorbance*; Eli Lilly & Company and the National Center for Advancing Translational Sciences: 2015. URL: <https://www.ncbi.nlm.nih.gov/books/NBK34329/>
- (23) Resch-Genger, U.; Hoffmann, K.; Niefeld, W.; Engel, A.; Neukammer, J.; Nitschke, R.; Ebert, B.; Macdonald, R. How to Improve Quality Assurance in Fluorometry: Fluorescence-Inherent Sources of Error and Suited Fluorescence Standards. *J. Fluoresc.* **2005**, *15*, 337–362.
- (24) Vacher, M.; Fdez Galvan, I.; Ding, B. W.; Schramm, S.; Berraud-Pache, R.; Naumov, P.; Ferre, N.; Liu, Y. J.; Navizet, I.; Rocas-Sanjuan, D.; Baader, W. J.; Lindh, R. Chemi- and Bioluminescence of Cyclic Peroxides. *Chem. Rev.* **2018**, *118*, 6927–6974.
- (25) Masson, E.; Shaker, Y. M.; Masson, J.-P.; Kordesch, M. E.; Yuwono, C. Supramolecular Circuitry: Three Chemiluminescent, Cucurbit[7]uril Controlled On/Off Switches. *Org. Lett.* **2011**, *13*, 3872–3875.
- (26) Wang, Q.; Li, L.; Xu, B. Bioinspired Supramolecular Confinement of Luminol and Heme Proteins to Enhance the Chemiluminescent Quantum Yield. *Chem. – Eur. J.* **2009**, *15*, 3168–3172.
- (27) Geiselhart, C. M.; Mutlu, H.; Tzvetkova, P.; Barner-Kowollik, C. Chemiluminescent Self-Reporting Supramolecular Transformations on Macromolecular Scaffolds. *Polym. Chem.* **2020**, *11*, 4213–4220.
- (28) Chen, L.; Chen, Y.; Zhou, W.; Li, J.; Zhang, Y.; Liu, Y. Mitochondrion-Targeting Chemiluminescent Ternary Supramolecular Assembly for In Situ Photodynamic Therapy. *Chem. Commun.* **2020**, *56*, 8857–8860.
- (29) Roda, A.; Guardigli, M. Analytical Chemiluminescence and Bioluminescence: Latest Achievements and New Horizons. *Anal. Bioanal. Chem.* **2011**, *402*, 69–76.
- (30) He, S.; Shi, W.; Zhang, X.; Li, J.; Huang, Y. Beta-Cyclodextrins-Based Inclusion Complexes of CoFe<sub>2</sub>O<sub>4</sub> Magnetic Nanoparticles as Catalyst for the Luminol Chemiluminescence System and Their Applications in Hydrogen Peroxide Detection. *Talanta* **2010**, *82*, 377–383.
- (31) Gnaim, S.; Scomparin, A.; Eldar-Boock, A.; Bauer, C. R.; Satchi-Fainaro, R.; Shabat, D. Light Emission Enhancement by Supramolecular Complexation of Chemiluminescence Probes Designed for Bioimaging. *Chem. Sci.* **2019**, *10*, 2945–2955.
- (32) Schaap, A. P.; Chen, T.-S.; Handley, R. S.; DeSilva, R.; Giri, B. P. Chemical and Enzymatic Triggering of 1,2-Dioxetanes. 2: Fluoride-Induced Chemiluminescence from Tert Butyldimethylsilyl xy-Substituted Dioxetanes. *Tetrahedron Lett.* **1987**, *28*, 1155–1158.
- (33) Gnaim, S.; Green, O.; Shabat, D. The Emergence of Aqueous Chemiluminescence: New Promising Class of Phenoxy 1,2-Dioxetane Luminophores. *Chem. Commun.* **2018**, *54*, 2073–2085.
- (34) Hananya, N.; Eldar Boock, A.; Bauer, C. R.; Satchi-Fainaro, R.; Shabat, D. Remarkable Enhancement of Chemiluminescent Signal by Dioxetane-Fluorophore Conjugates: Turn-ON Chemiluminescence Probes with Color Modulation for Sensing and Imaging. *J. Am. Chem. Soc.* **2016**, *138*, 13438–13446.
- (35) Cao, J.; Campbell, J.; Liu, L.; Mason, R. P.; Lippert, A. R. In Vivo Chemiluminescent Imaging Agents for Nitroreductase and Tissue Oxygenation. *Anal. Chem.* **2016**, *88*, 4995–5002.
- (36) Adam, W.; Reinhardt, D.; Saha-Moiler, C. R. From the Firefly Bioluminescence to the Dioxetane based (AMPPD) Chemiluminescence Immunoassay: a Retroanalysis. *Analyst* **1996**, *121*, 1527–1531.
- (37) Matsumoto, M. Advanced Chemistry of Dioxetane-Based Chemiluminescent Substrates Originating from Bioluminescence. *J. Photochem. Photobiol. C: Photochem. Rev.* **2004**, *5*, 27–53.
- (38) Bronstein, I.; Edwards, B.; Voyta, J. C. 1,2-Dioxetanes: Novel Chemiluminescent Enzyme Substrates. Applications to Immunoassays. *J. Biolumin. Chemilumin.* **1989**, *4*, 99–111.
- (39) Hananya, N.; Shabat, D. Recent Advances and Challenges in Luminescent Imaging: Bright Outlook for Chemiluminescence of Dioxetanes in Water. *ACS Cent. Sci.* **2019**, *5*, 949–959.
- (40) Green, O.; Eilon, T.; Hananya, N.; Gutkin, S.; Bauer, C. R.; Shabat, D. Opening a Gateway for Chemiluminescence Cell Imaging: Distinctive Methodology for Design of Bright Chemiluminescent Dioxetane Probes. *ACS Cent. Sci.* **2017**, *3*, 349–358.
- (41) Schaap, A. P.; Akhavan, H.; Romano, L. J. Chemiluminescent Substrates for Alkaline Phosphatase: Application to Ultrasensitive Enzyme-Linked Immunoassays and DNA Probes. *Clin. Chem.* **1989**, *35*, 1863–1864.
- (42) Partearroyo, M.; Ostolaza, H.; Goñi, F. M.; Barberá-Guillem, E. Surfactant-Induced Cell Toxicity and Cell Lysis. *Biochem. Pharmacol.* **1990**, *40*, 1323–1328.
- (43) Prabodh, A.; Sinn, S.; Grimm, L.; Miskolczy, Z.; Megyesi, M.; Biczók, L.; Bräse, S.; Biedermann, F. Teaching Indicators to Unravel the Kinetic Features of Host-Guest Inclusion Complexes. *Chem. Commun.* **2020**, *56*, 12327–12330.
- (44) Liu, J.; Jiang, J.; Dou, Y.; Zhang, F.; Liu, X.; Qu, J.; Zhu, Q. A Novel Chemiluminescent Probe for Hydrazine Detection in Water and HeLa cells. *Org. Biomol. Chem.* **2019**, *17*, 6975–6979.
- (45) Miskolczy, Z.; Biczók, L.; Lendvay, G. Substituent Effect on the Dynamics of the Inclusion Complex Formation Between Protoberberine Alkaloids and Cucurbit[7]uril. *Phys. Chem. Chem. Phys.* **2018**, *20*, 15986–15994.
- (46) Watanabe, N.; Takatsuka, H.; Ijuin, H. K.; Matsumoto, M. Highly Effective and Rapid Emission of Light from Bicyclic Dioxetanes Bearing a 3-Hydroxyphenyl Substituted with a 4-p-OligoPhenylene Moiety in an Aqueous System: Two Different Ways for the Enhancement of Chemiluminescence Efficiency. *Tetrahedron* **2020**, *76*, No. 131203.
- (47) Lazar, A. I.; Biedermann, F.; Mustafina, K. R.; Assaf, K. I.; Hennig, A.; Nau, W. M. Nanomolar Binding of Steroids to Cucurbit[n]urils: Selectivity and Applications. *J. Am. Chem. Soc.* **2016**, *138*, 13022–13029.
- (48) Robinson, D. M.; Keating, G. M. Memantine A Review of its Use in Alzheimer's Disease. *Drugs* **2006**, *66*, 1515–1534.

- (49) Wu, C.; Kovac, J. R. Novel Uses for the Anabolic Androgenic Steroids Nandrolone and Oxandrolone in the Management of Male Health. *Curr. Urol. Rep.* **2016**, *17*, 72.
- (50) Sakamoto, S.; Putalun, W.; Vimolmangkang, S.; Phoolcharoen, W.; Shoyama, Y.; Tanaka, H.; Morimoto, S. Enzyme-Linked Immunosorbent Assay for the Quantitative/Qualitative Analysis of Plant Secondary Metabolites. *J. Nat. Med.* **2018**, *72*, 32–42.
- (51) Nagasawa, S.; Yajima, D.; Torimitsu, S.; Chiba, F.; Iwase, H. Postmortem Memantine Concentration in a Non-Intoxication Case, and the Possibility of Postmortem Redistribution: A Case Report. *Forensic Sci. Int.* **2015**, *257*, e12–e15.
- (52) Klein-Schwartz, W.; Oderda, G. M. Poisoning in the Elderly. *Drugs Aging* **1991**, *1*, 67–89.
- (53) Kohler, R. M. N.; Lambert, M. I. Urine Nandrolone Metabolites: False Positive Doping Test? *Br. J. Sports. Med.* **2002**, *36*, 325–329.
- (54) Kricka, L. J. Clinical Applications of Chemiluminescence. *Anal. Chim. Acta* **2003**, *500*, 279–286.
- (55) Hu, C.; Grimm, L.; Prabodh, A.; Baksi, A.; Siennicka, A.; Levkin, P. A.; Kappes, M. M.; Biedermann, F. Covalent Cucurbit[7]-uril-Dye Conjugates for Sensing in Aqueous Saline Media and Biofluids. *Chem. Sci.* **2020**, *11*, 11142–11153.
- (56) Zhang, S.; Grimm, L.; Miskolczy, Z.; Biczók, L.; Biedermann, F.; Nau, W. M. Binding Affinities of Cucurbit[n]urils with Cations. *Chem. Commun.* **2019**, *55*, 14131–14134.
- (57) Zhang, S.; Assaf, K. I.; Huang, C.; Hennig, A.; Nau, W. M. Ratiometric DNA Sensing with a Host-Guest FRET pair. *Chem. Commun.* **2019**, *55*, 671–674.
- (58) Dong, N.; He, J.; Li, T.; Peralta, A.; Avei, M. R.; Ma, M.; Kaifer, A. E. Synthesis and Binding Properties of Monohydroxycucurbit[7]-uril: A Key Derivative for the Functionalization of Cucurbituril Hosts. *J. Org. Chem.* **2018**, *83*, 5467–5473.
- (59) Kamel, F. Paths from Pesticides to Parkinson's. *Science* **2013**, *341*, 722–723.
- (60) Vermeulen, L. A.; Thompson, M. E. Stable Photoinduced Charge Separation in Layered Viologen Compounds. *Nature* **1992**, *358*, 656–658.
- (61) Jagadesan, P.; Valandro, S. R.; Schanze, K. S. Ultrafast Photoinduced Electron Transfer in Conjugated Polyelectrolyte–Acceptor Ion Pair Complexes. *Mater. Chem. Front.* **2020**, *4*, 3649–3659.